Microchim Acta (2015) 182:933–942
DOI 10.1007/s00604-014-1413-4

ORIGINAL PAPER

Voltammetric sensor for theophylline using sol–gel immobilized molecularly imprinted polymer particles

Ferdia Bates · Manel del Valle

Received: 1 August 2014 / Accepted: 10 November 2014 / Published online: 19 November 2014

Abstract Sensors incorporating molecularly imprinted polymers (MIPs) are feasible in concept though the reproducibility of such devices can be compromised by the large number of interdependent steps. For this reason, many researchers have focused on the synthesis of MIP particles only, not on their immobilization. Herein is presented a sol–gel based method for immobilization of unmodified MIP particles for use in an electrochemical sensor. The macroporous particles were prepared using precipitation-polymerization and imprinted with theophylline. The sol–gel was combined with graphite microparticles (50 μm) and the composite was deposited on the surfaced of an epoxy-graphite electrode. The sensor was then tested for its response to theophylline using differential pulse voltammetry. A limit of detection of 1 μM was observed and a relative standard deviation of 6.85 %. The electrode can be regenerated via a thermal washing process which was accompanied by an initial signal loss of 29.3 %. Any further regeneration caused a signal loss of 2.4 % only.

Keywords Molecularly imprinted polymers (MIP) · Sol–gel · Graphite · Theophylline · Differential pulse voltammetry

Introduction

The necessity for novel qualitative sensor systems with the capacity to detect targeted molecular compounds is ever-present. For several decades, sensors based on biological recognition, such as those utilizing enzymes, antibodies, microorganisms or aptamers, have received a majority of interest within this field thanks to their superior recognition properties [1]. Biomolecules do, however, suffer from a generally poor chemical and physical stability as well as being costly to synthesize or refine and thus in more recent years, artificial receptors have been garnered with an increasing degree of attention [2].

Molecular imprinting embodies the creation of a tailored binding site for a selected template molecule. The binding sites that are created can be highly specific and have the ability to discriminate between structurally similar compounds as well as chiral molecules [3]. This field is most commonly manifested in the paradigm of Molecularly Imprinted Polymers (MIPs) which has exhibited exponential growth with respect to annual publications over the course of the last two decades [4]. Though there are two main imprinting strategies, covalent and non-covalent, the non-covalent approach is afforded greater attention due to the speed and ease of synthesis, facile post-binding regeneration and the greater level of functionality at the binding site [5]. The synthesis of such MIPs, generally consists of a preassembly step whereby the template molecule is mixed with a functional monomer to form complexes with the template at its local dipoles. The spatial orientation of these binding sites is then secured via the crosslinking of the functional monomer with a secondary copolymer, which fixes at proper distance and geometry the binding sites; at this point, the template can be extracted from the newly-formed cavities [6] and usages of the MIP can developed; a schematic of this process, using theophylline as a template, can be seen in Fig. 1. The popularity of MIPs comes from their low cost, ease of preparation and high stability [7]; these attributes have garnered them with the title ‘plastic antibodies’ [8].

Given their advantages, molecular imprinting appears equally enticing to laboratories regardless of the level of in-house synthetic expertise. There are, however, some drawbacks and discouragements while attempting to imprint polymers. Of the two most common structural forms of MIPs,

F. Bates · M. del Valle (✉)
Sensors and Biosensors Group, Department of Chemistry,
Universitat Autònoma de Barcelona, Bellaterra,
Barcelona 08193, Spain
e-mail: manel.delvalle@uab.es

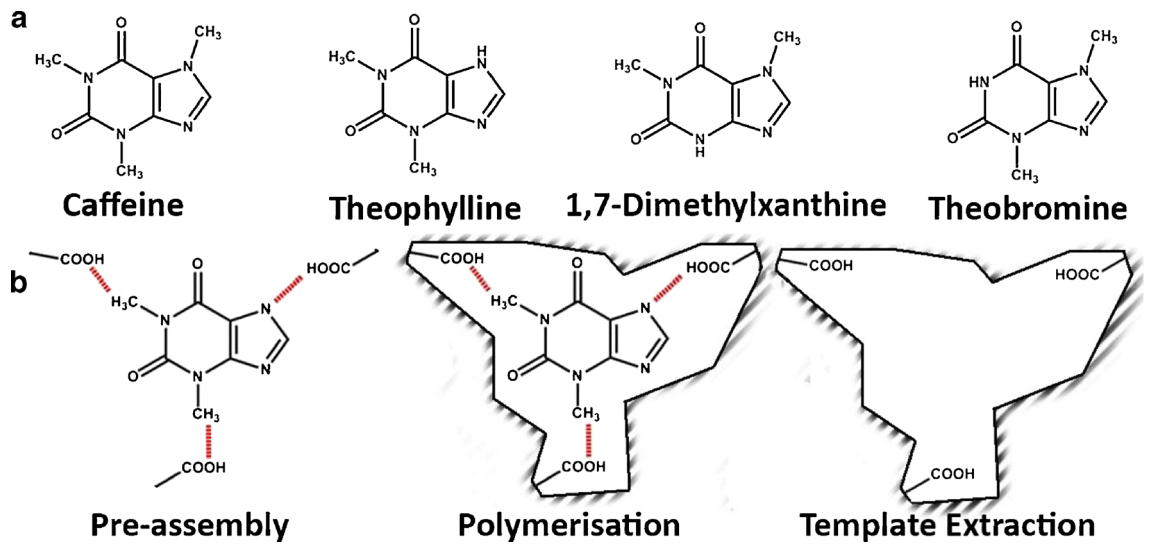

Fig. 1 Molecular structure of caffeine, theophylline theobromine and 1,7-dimethylxanthine (**a**); schematic of the creation of a theophylline-imprinted binding site consisting of the pre-assembly of the functional monomer and the template, polymerization of the crosslinking polymer and the subsequent removal of the template to leave a functional binding site (**b**)

particles and deposited films, both are accompanied by disadvantages which hinder the exploitation of molecular imprinting as an analytical technique. While particles are easier to synthesize compared to films [9], the number of immobilization methods for MIP particles available in the literature is limited. This low level of available protocols can be noticed as those referenced in a 2010 review of the state-of-the-art of molecular imprinting in electrochemistry [10]. Of 61 papers reporting the immobilization of MIPs onto sensors only five of these, less than 10 %, employed unmodified MIP particles as the sensing mechanism Four additional citations reported the use of packed columns or flow systems though such strategies suffer from drawbacks of slow rebinding of the target within the cavities of the MIP, leading to long extraction times [11].

Theophylline, the molecule chosen as molecular template for this work, is a methylxanthine alkaloid of the purine family and is present in cocoa beans, teas and a range of other beverages and plant materials along with its structural analogues caffeine and theobromine. For over 70 years it has been used to treat maladies of the airway such as asthma and chronic obstructive pulmonary disease (COPD). Its low cost and high availability have both contributed to make it one of the most widely prescribed drugs for such pathologies [12]. Its simple structure and close similarity to its analogues (Fig. 1) make it an attractive molecule to study in the field of molecular imprinting. Its low cost and toxicity also increases the attraction of using it in prototype studies [13, 14].

Conventional methods for the detection of methylxanthines are based on gas and liquid chromatography, the advantages of which are clouded by the requirement of bulky, expensive equipment, complicated sample pretreatments and trained operators to run the analysis [15, 16]. Electrochemical methods on the other hand, embodied by voltammetric, potentiometric, amperometric and piezoelectric devices, were until relatively recently not commonly used for their detection [17]. This is due to their extremely high oxidation potentials, observed with common electrochemical systems incorporating metallic and/or carbon-based electrodes, which make the final signal poorer, with background noise created from oxidative currents and limited reproducibility [13, 18].

Synthesis techniques of particulate MIPs consist of bulk, suspension, emulsion, two-step swelling and/or precipitation polymerizations [19]. The disadvantage of bulk imprinting, the most commonly used technique, lies in the high volume of material and template that is required by the synthesis. The monolith particles obtained can also have a low capacity due to binding-site heterogeneity and poor site accessibility stemming from the grinding process needed to break the polymer brick [20], thus there is a need to investigate alternative synthesis strategies.

Though MIPs have already been successfully applied to the majority of the contemporary transduction mechanisms [21], there is instead a deficit in the availability of facile immobilization methods for particulate MIPs onto the surface of available transducers for rapid sensing of the targeted molecule; such methods would allow for the rapid substitution of the molecule targeted by the sensor via a change in the imprinted template rather than the laborious redesign of the sensor, thus greatly increasing the versatility of the systems.

The key difficulty in the search for an effective immobilization method for particulate MIPs lies in the compromise between extraction or measurement time and reproducibility. When using monolithic MIP particles, a large quantity must be used in order to negate the potential heterogeneity of the measurement due to the aforementioned accessibility issues. When such particles are immobilized in lower quantities, in a

membrane for example, the decreased availability of the binding sites lead to undesirably high variability between measurements [14]. Incorporation of the monoliths inside the electrode increases the robustness of the sensor and allows the use of more aggressive strategies to be used for signal amplification [13] though this method does not allow for the removal of the template upon re-binding and thus effective regeneration of the sensor is not possible.

Though the use of an agarose membrane for the immobilization of MIP particles onto a sensor surface is well documented [20, 22], it was rejected due to the slow response time with respect to membrane thickness, an increase of which is required with respect to increased oxidation potential of analyte. Also, the complete coverage of the MIP particles by a membrane would also negate the possibility of electrode regeneration.

Sol–gel immobilized MIPs have been reported in which high voltage potentials (1.4–2.0 V) are incorporated into the sensing [23]. Further work by the same laboratory immobilizes hyper-branched MIP particles inside an identical sol–gel membrane [24]. While the non-conventional imprinting strategy employed, known as the Takagishi method is effective [25], the elevated temperatures used during the polymerization process renders it unsuitable for imprinting many organic molecules. It should also be noted that it is also possible to imprint directly into a sol–gel matrix, using its polymeric structure to replace one or both of the functional and crosslinking monomers [26] though this strategy was also rejected in favour of maintaining the segregation between the imprinting and immobilization events.

In this work, a theophylline-imprinted polymer-incorporating voltammetric sensor is presented. Microspherical macroporous MIP particles were immobilized using the sol–gel technique together with graphite as the conducting medium on the surface of a carbon electrode. The theophylline-imprinted polymer was synthesized using standard protocols of precipitation polymerisation and their morphology and size distribution was confirmed via Scanning Electron Microscopy (SEM). Prepared sol–gel membranes were also characterised using confocal microscopy. Primary response and electrode regeneration was investigated using adsorptive stripping voltammetry (ASV) employing the differential pulse technique. Cross response to other methylxanthines: 1,7-dimethylxanthine, caffeine and theobromine was fully characterised. The limit of detection of the electrode was also demonstrated using chronoamperometry.

Experimental

Reagents and chemicals

50 μm particle size graphite powder (Merck, Darmstadt, Germany; http://www.merck.com/) was used in the preparation of the sol–gel membranes and of the epoxy-graphite electrodes. Epotek H77 resin and its corresponding hardener (Epoxy Technology, Billerica, MA, USA; http://www.epotek.com/) were also used in the electrode fabrication. All reagents were analytical reagent grade. All solvents were purchased from Scharlab, (Scharlab, Barcelona, Spain; http://www.scharlab.com/). 1,7-dimethylxanthine, theophylline, theobromine, caffeine, methacrylic acid (MAA), ethylene glycol dimethyl acrylate (EGDMA) and tetraethyl orthosilane (TEOS) were purchased from Sigma-Aldrich (Sigma-Aldrich, St. Louis, MO; https://www.sigmaaldrich.com/). The radical initiator 2,2'-Azobis (2,4-dimethylvaleronitrile) (AIVN) was purchased from Wako Chemicals GmbH (Wako Chemicals GmbH, Neuss, Germany; http://www.wako-chemicals.de/). All other acids and potassium hydrogen phthalate were purchased from Panreac (Panreac, Barcelona, Spain; http://www.panreac.es/).

Apparatus

All polymerisations were done in a water bath controlled with a Huber CC1 thermoregulation pump (Huber Kaeltemaschinenbau GmbH, Offenburg, Germany; http://www.huber-online.com/). All experiments were conducted using a commercial 52–61 platinum combined Ag/AgCl reference and counter electrode (Crison Instruments, Barcelona Spain; http://www.crisoninstruments.com/). All voltammetric measurements were carried out using a DropSens μStat8000 multi-potentiostat/galvanostat and processed using Dropview 8400 computer software (Dropsens, Oviedo, Spain; http://www.dropsens.com/). Chronoamperometry measurements were executed using an Autolab PGStat 20 (Metrohm Autolab B.V, Utrecht, The Netherlands; http://www.ecochemie.nl/). SEM analysis was executed using a MERLIN FE-SEM (Zeiss GmbH, Jena, Germany; http://www.zeiss.com/). Confocal microscopy was done with a Leica DCM-3D system (Wetzlar, Germany; http://www.leica-microsystems.com/).

Preparation of theophylline-imprinted polymer particles

The protocol for the precipitation polymerisation synthesis of the MIP particles was taken from the literature [27]. In brief, inhibitor in the MAA and EGDMA was removed immediately prior to use via passage through separate inhibitor removal columns (Sigma-Aldrich, St. Louis, MO; https://www.Sigmaaldrich. com/). 0.255 mmol of Theophylline was combined with 0.911 mmol of MAA in 40 mL of acetonitrile in a round bottomed flask. The mixture was then stirred gently at low temperature for 10 min. 3.64 mmol of EGDMA and 0.0852 mmol of AIVN were then added and mixed briefly. The solution was sonicated under vacuum and then purged with nitrogen for 10 min, at which point the flask

was sealed and placed in a 60 °C water bath for 16 h. A control non-imprinted polymer was also created using an identical procedure with the omission of theophylline. The MIP particles were then removed from the porogen via centrifugation at 4500 RPM for 10 min and then equally divided between three 15 mL Falcon tubes. The particles were washed using 10 mL of 9:1 methanol: acetic acid solution for 1 h, at which point the washing solvent was refreshed; next, the tubes were centrifuged and the supernatant replaced. This process was repeated 5 times to ensure the complete removal of the template molecule; the particles were then rinsed again with methanol only and dried in an oven at 70 °C.

Electrode preparation and MIP-sol–gel immobilization and regeneration

The electrodes used for experimentation were epoxy-graphite composite electrodes of normal use in the laboratory of the authors and were prepared using a previously published in-house protocol with a final geometric surface area of 0.28 mm^2 [28]. Following the curing duration, the electrodes were wet-polished with 400 grit abrasive-paper and degreased with acetone. The immobilization of the MIP particles onto the surface of the epoxy-graphite electrode was modified from a previously published protocol [29]. 0.5 mL TEOS, 0.5 mL ethanol, 0.25 mL water and 25 μL of 0.1 M hydrochloric acid (HCl) were combined and stirred vigorously for 35 min and rested for approximately 45 min to arrive at the syneresis stage. This liquid was combined with graphite and a MIP-DMF suspension in the ratio 200 μL to 7 mg to 40 μL respectively. The MIP-DMF suspension consisted of 15 mg of MIP particles and 1 mL of DMF; the experimental control consisted of particles polymerised in the absence of the template, a non-imprinted polymer (NIP). This mixture was shaken for 10 min at 1400 RPM. 10 μL of this solution was deposited in the centre of each electrode and evenly distributed via a home-made spin coater at 1400 RPM for 60 s. The electrodes were dried at atmospheric pressure at 5 °C overnight and conditioned in water for 1 h before use. For regeneration experiments, the electrodes were immersed in 0.05 M HCl at 60–65 °C for 10 min and then conditioned in water for 1 h before subsequent use.

Electrochemical measurements

Differential Pulse Voltammetry in all experiments was performed with a scan range between 1 and 1.7 V, a pulse potential of 0.01 V, duration of 300 ms and a scan rate of 0.04 $V \cdot s^{-1}$. A base line measurement was taken at t=0 (t_0) from which all proceeding measures were subtracted. Chronoamperometry experiments were performed at +1.18 V. All measurements were done in pH=3 phthalate buffer with the pH adjusted using 0.1 M HCl. An accumulation time of 5 min was used in all experiments unless otherwise stated whereby the electrode was immersed in the analyte ahead of the measurement event.

Results and discussion

Particle synthesis and sol–gel immobilization

Precipitated microspheres were used for sol–gel immobilization due to their small size and high homogeneity. The synthesis protocol used employed a molar ratio of 1:4 MAA: EGDMA to ensure high crosslinking and optimal rigidity to maintain binding-site morphology within the polymer matrix.

The yield following template removal was 563 mg, calculated as an efficiency of 64 % by weight, 24 % less than that given by Ye et al. [27]. This drop in yield efficiency is speculated to originate in the lower centrifugation speeds used during the template removal process. SEM analysis confirmed the formation of highly uniform spherical particles (Fig. 2a and b). A superficial roughness or 'wrinkled' aspect was observed on the surface of the polymers; an advantageous feature of macroporous particles due to the increment in surface area it provides. This surface area is permanent both in the dry state and is not susceptible to solvent-related swelling, a feature of traditional monolith MIPs which can place stress on both the polymer and the supporting matrix, a phenomenon which can affect rebinding performance [30]. A subsequent statistical analysis (Fig. 2c) found the particle size distribution to be in keeping with that published in the literature. 54 % of the particle yield was made up of sizes at 970 nm while 96 % of the yield was above 665 nm. In contrast to the large positive skew seen in the distribution of the MIP particle synthesis, the NIP control saw a quite narrow (σ= 33.1 nm), normal distribution of particle sizes; with 46 % of the yield being sized at the mean value and 86 % of the total being at or above the mean of 116 nm, shown in Fig. 2d.

The greatly diminished particle size demonstrates the sensitivity of precipitation polymerisation protocols to the choice of template due to the augmented solubility parameter which the presence of the template, theophylline, provides relative to the control. In brief, the solubility parameter is a term in polymer chemistry used to describe solvent-monomer compatibility based on the absolute sum total of the dipole-dipole, hydrogen bond and dispersion forces between the solvent and the dissolved monomer (s). When polymerisation is induced, the resultant chain becomes progressively more unstable until the point of phase separation which causes the collapse and subsequent precipitation of the polymer chain into the solvent and thus the formation of a polymer particle. In the case of MIPs, the additional polar surface area of the template molecule provides substantial additional thermodynamic stability during chain growth which can significantly delay polymer

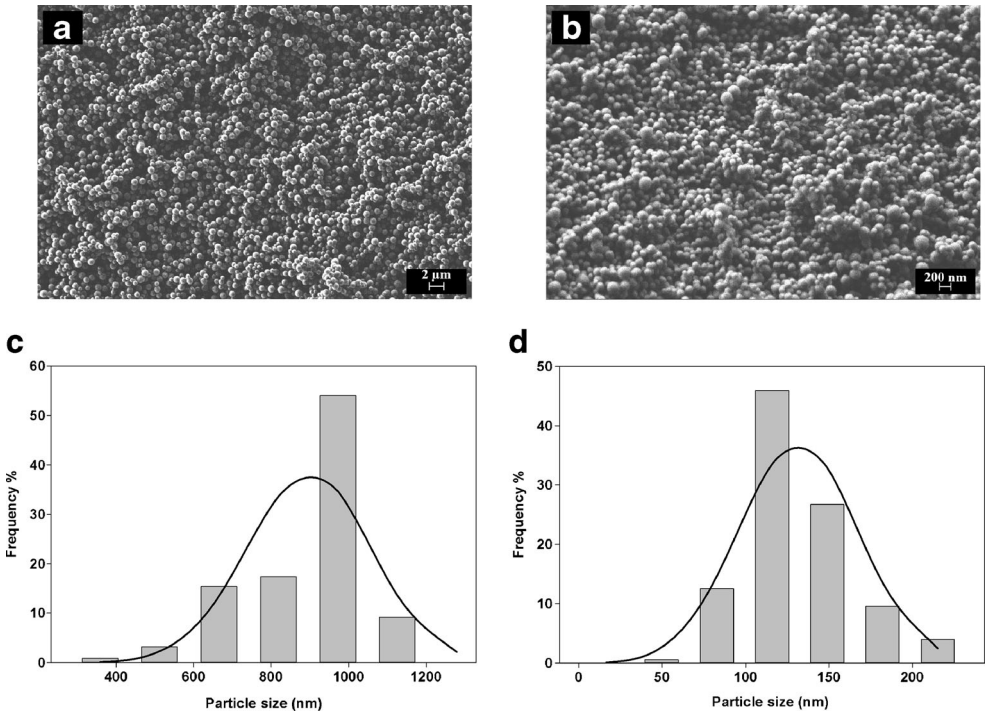

Fig. 2 SEM of uniform spherical Theophylline-Imprinted Polymer particles (**a**) and the NIP control (**b**); Statistical analysis of MIP particle size distribution with a mean of 819 nm and standard deviation of 153 nm (**c**) and statistical analysis of NIP particle size distribution with a mean of 116 nm and standard deviation of 33 nm (**d**)

precipitation into the solvent phase, resulting in a large size difference between the MIP and its control [31, 32]; in this case, this size difference is 7-fold. The increase in particle size distribution observed in the MIP relative to its control can be minimised with decreased mechanical agitation, which is the main source of turbulence within the solvent phase during the polymerisation process.

Optimisation and determination of deposition, drying and regeneration sol–gel conditions

In order to obtain a sensing surface usable for voltammetry, it was decided to immobilize the obtained MIP microspheres within a sol–gel matrix. This was done by modifying a procedure determined by Patel et al. [23, 29, 33, 34]. Optimal results were seen when the electrodes were chilled immediately following the deposition and distribution (spin coating) and allowed to dry over night at ambient pressure. Though signal intensity was seen to be related to the final gel thickness, an optimised deposited volume of 10 μL on the graphite-epoxy composite electrode was chosen as larger deposition volumes were seen to increase the instance of crack formation on the gel surface, a finding consistent with the literature [35]. Though it is possible to negate the instance of crack altogether as well as to achieve extremely high film uniformity via multiple layered depositions [36], the signal augmentation that was seen with the single deposition was not replicated when multiple layers were built up on the electrode surface. The use of high-potential voltammetric cycling or sustained high voltage pre-treatments were seen to be detrimental to the structural integrity of the sol–gel and thus obliged the subtraction of interfering background currents prior to each measurement. Performance of measurements in strong acids in order to increase the signal to noise ratio, as used for the detection of similar compounds [13], also was not feasible as the acid caused the gel deterioration due to continued hydrolysis of the sol–gel membrane.

To elaborate on the choice made for buffer pH, theophylline exhibits a sharp approximately linear increase in oxidative current with acidifying pH values [18]. However, with respect to the MIP recognition element, this augmentation in signal intensity can only be exploited until a point before the degree of ionisation of the target molecule in the buffer renders it unfit for the imprinted cavity and thus dropping selectivity [24]; high relative standard deviation (RSD) also occurs when detection is attempted at pH values too close to the pK_a of the target. Accordingly, pH 3 was chosen as the detection pH sufficiently distanced from the dissociation points of theophylline given as 5.6 and 2.5 [37]. The use of such a buffer combines the binding and signal augmentation requirements to allow for a facile single step detection process without losing the imprinting effect of the MIP relative to its control.

Upon deposition, the sol mixture was evenly distributed using a home-made spin coater. When dried, the thickness of the membrane was measured using a 3D confocal microscope (Fig. 3a). It was observed that though the greatest thickness remained at the centre of the electrode at the site of the deposition, the overall distribution of membrane thickness was relatively uniform varying from approximately 200 μm at the extreme peripheries of the electrode to 300 μm at the

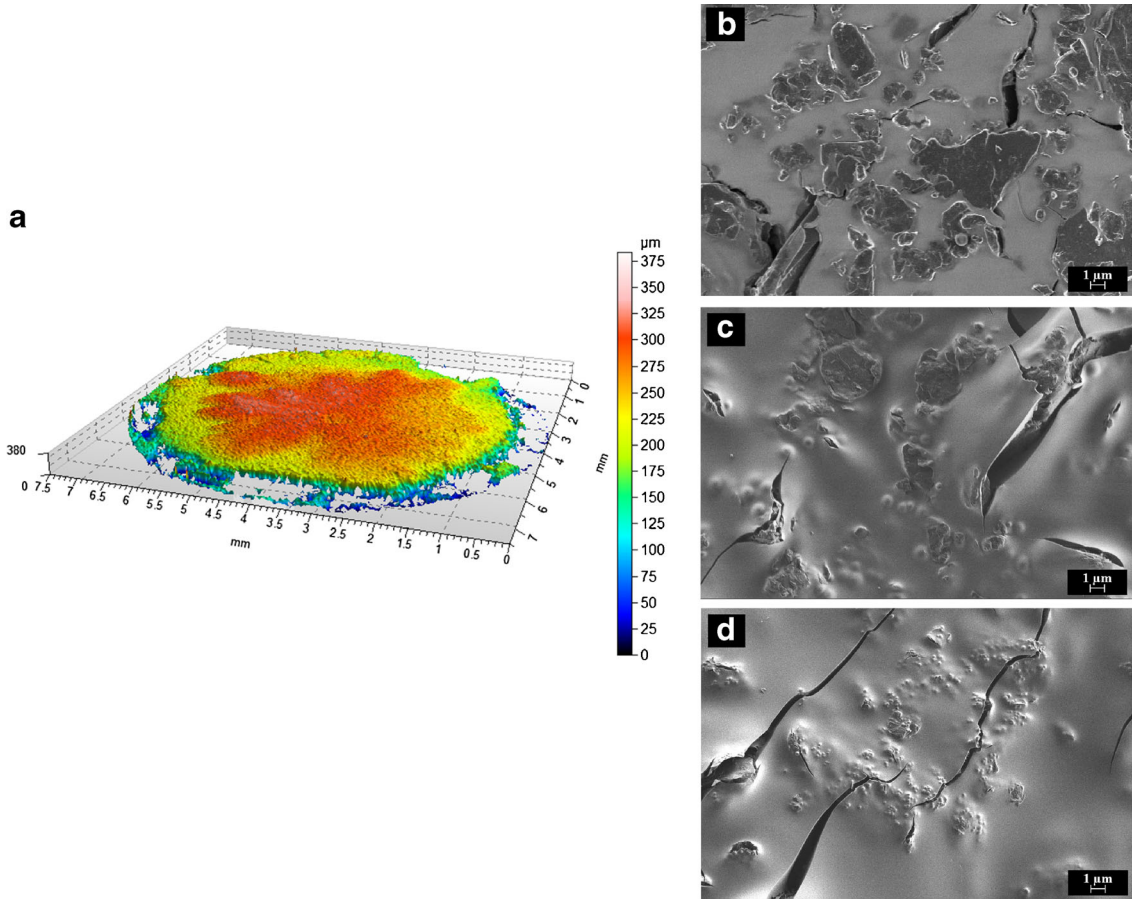

Fig. 3 3-dimensional surface profile and film-thickness of sol–gel on electrode surface obtained by confocal microscopy examination (**a**); SEM images of a deposited sol–gel membranes containing graphite only (**b**) and the sol–gel immobilized MIP and NIP microspheres (**c & d**)

original deposition point. This variation was seen to arise from the decrease in solution thickness, as well as graphite particle quantity, which occurred when the graphite particle size was increased while the mass proportion remained constant; this fact decreasing the in-situ availability of the graphite causing a substantial gradient to be observed. Increasing the mass proportion of the graphite in order to compensate this reduction, though aiding in the homogeneous distribution of the gel upon disposition, provoked an increased incidence of crack formation in the sol–gel surface upon drying; this obliged a reduction in deposition volume and decreased signal strength.

It was seen that the MIP particles preferentially occupied the surface of the sol–gel electrode, clustering around the graphite particles (Fig. 3b–d). This orientation is advantageous as it reduces the incidence of non-specific interactions between the analyte solution and the graphite particles and thus maximises the specific binding events between the MIP particles and the target analyte. The high availability of the MIP particles at the surface of the sensor also allows for a reduction in the immersion time in the analyte required before measurement can occur as well as allowing the sensor to be regenerated as will be discussed below.

The volume of MIP particles in the sol–gel membrane was determined through varying their concentration in the MIP-DMF suspension that was used during the synthesis of the sol–gel membrane (Fig. 4). It was found that 15 mg/mL caused the greatest augmentation in signal strength for the MIP-sol–gel electrode after which point the insulating effect of the methacrylate particles overrode the imprinting effect of the MIP. Interestingly, a linear decrease in oxidation potential was observed with respect to polymer concentration in the sol–gel. In the case of theophylline this decrease was from +1.22 V the lowest concentrations tested (0–7.5 mg·mL^{-1}) to +1.09 V for the highest (30 mg·mL^{-1}).

Electrochemical characterization

The devised theophylline sensor made by the immobilization of MIP microspheres in a sol–gel matrix was subsequently used in adsorptive stripping voltammetric determination of the alkaloid using DPV. A baseline was taken at t_0 so as to negate any nonspecific interactions between the graphite support and the analyte; all subsequent measurements were subtracted from this initial level. An accumulation time of 5 min was

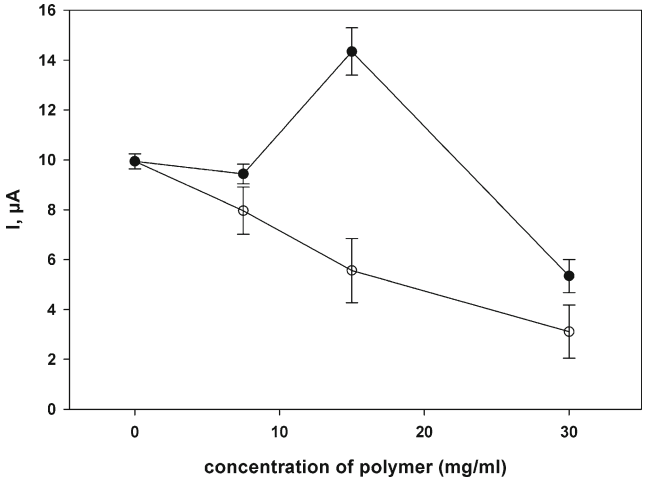

Fig. 4 Optimisation of the concentration of polymer particles in the MIP-DMF suspension used in the synthesis of the MIP-sol–gel membrane (●) and NIP-sol–gel control electrode (○) up to 30 mg/mL for 0.27 mmol of theophylline

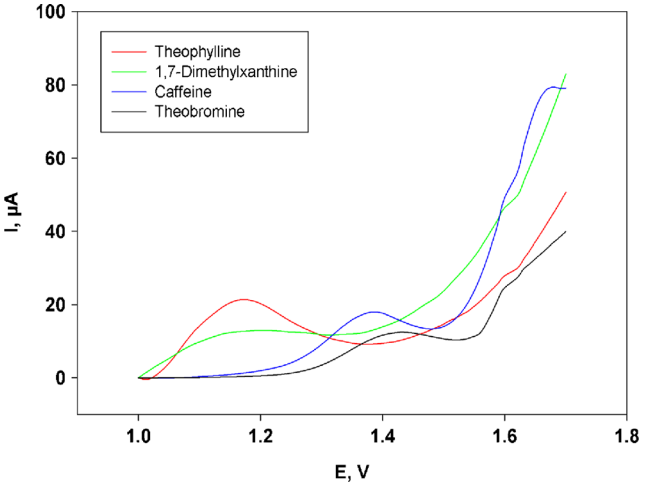

Fig. 6 DPV voltammograms of the MIP-sol–gel electrode for caffeine, theophylline, theobromine and 1,7-dimethylxanthine at a concentration of 0.27 mmol·L^{-1}, t=5 min, range 1–1.7 V, a pulse duration of 300 ms, pulse potential of 0.01 V and scan rate of 0.04 V·s^{-1}

chosen for measurements due to the minimal signal increase which occurred thereafter; additionally, this low increase was accompanied by an increased inter-electrode signal heterogeneity causing a substantial rise in RSD (Fig. 5).

When different methylxanthines were assayed with the prepared electrode, oxidation peaks of +1.14, +1.18, +1.36 and +1.4 V were observed for 1,7-dimethylxanthine, theophylline, caffeine and theobromine respectively (Fig. 6). An increase in oxidative peak width observed in the MIP-sol–gel electrode is due to a decrease in the rate of electron transfer, a problem synonymous with sensors incorporating non-conductive monomers. Though oxidation peaks can be sharpened by reducing the scan rate used, this in turn increases the duration of measurement and cannot be an ultimate solution to this phenomenon [23]; the peak width is in keeping with other voltammetric MIP-incorporating systems [13].

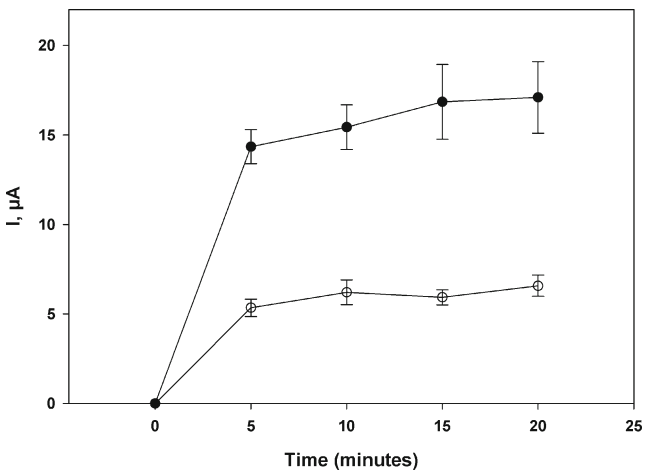

Fig. 5 Dynamic response of MIP-sol–gel electrode (●) and NIP-sol–gel control electrode (○) toward the primary imprinted methylxanthine (Theophylline) in a pH=3 phosphate buffer solution at a concentration of 0.27 mmol·L^{-1}

Current intensities were extracted from the profiles by subtracting the background signal and averages were made (n=5). RSD was calculated as 6.85 % for the primary target and an intensity of 258.1 % (relative to control NIP-sol–gel electrode) (Fig. 7). Lesser differentiation was seen between 1,7-dimethylxanthine, caffeine and theobromine which yielded intensities being only 168.1, 125.6 and 119.7 % with respect to their controls. Though uric acid, acetaminophen, ascorbic acid and glucose were also tested, no oxidation peaks were produced within the measurement range, demonstrating a reduced interference from non-xanthine compounds.

Regeneration of the MIP-sol–gel immobilized electrode was attempted. The temperature of 60–65 °C, duration of 10 min, and acidic strength of 0.05 M HCl, were optimised. Similar to that found during the optimisation of the deposition

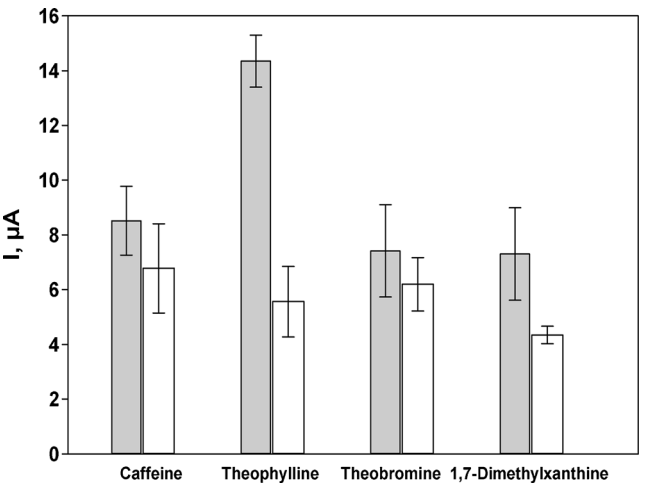

Fig. 7 Oxidation peak heights of the MIP-sol–gel electrode (solid bars) and NIP-sol–gel electrode (*white bars*) for caffeine, theophylline, theobromine and 1,7-dimethylxanthine at an analyte concentration of 0.27 mmol·L^{-1}

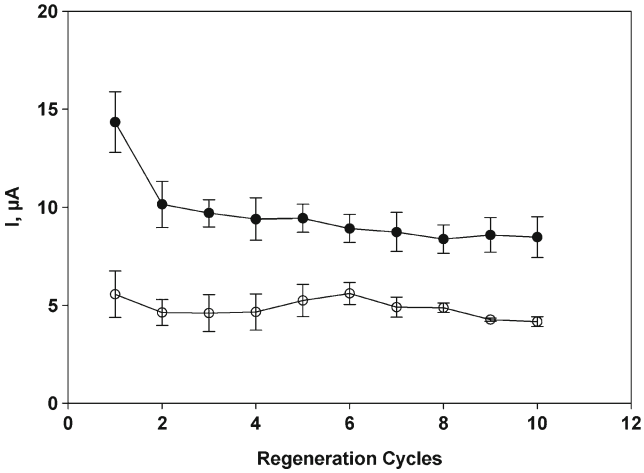

Fig. 8 Regeneration of MIP-sol–gel electrode (●) and NIP-sol–gel control electrode (○) using thermal-acidic treatment calculated from n= 5 replications

of the gel, strong acid and sustained augmented temperatures were detrimental to the integrity of the sol–gel structure; thus the parameters were determined. It was also seen that use of the electrode immediately following regeneration caused erratic results; this is believed to be due to the electrode body acting as a thermal battery, thus a relaxation period was required to return the electrodes to a base level.

As was observed by Alizadeh et al. [13], measures subsequent to the initial binding event decreased in intensity. Such was the behaviour seen in the MIP-sol–gel electrode whereby all measures following the first were approximately 70.7 % of the initial measurement (Fig. 8). It was seen, however, that the linear pattern seen from the first regeneration cycle one was consistent for up to 40 regeneration cycles (not shown) with an average signal loss of 2.35 % per cycle. The initial 29.3 % decrease, is due to the occupation of the deeply-seated, high affinity binding sites within the MIP particle structure which cannot be completely cleaned following the initial binding event. This decrease from the initial signal intensity could be reduced with the use of a MIP synthesized via photo-activated polymerisation rather than thermal polymerisation; this would greatly increase the number of lower affinity binding sites; such sites would be suitable for template recognition whilst also facilitating a more thorough regeneration of the sensor though conversely, could reduce the accuracy of the resulting sensor by facilitating secondary structural analogues to bind in these lower energy sites [38]. The subsequent preferential recognition of the analyte exhibited by the MIP-sol–gel electrode can be attributed to binding sites located on the aforementioned 'wrinkled' surface of the particles. The efficacy of the regeneration of the sensor hinges on the use of macroporous microparticles, rather than bulk-polymerised monoliths, whereby a permanent and heterogeneous pore structure allows the unhindered removal of the template from the binding sites on the particle surface.

The limit of detection (LOD) of the sol–gel immobilized MIP was seen to be 1 μM ($y=53.436x+0.0053$; $R^2=0.984$), consistent with the LODs of conductive sensors employing similarly synthesised un-specialised MIP particles as well as being in keeping with other contemporary electrochemical systems for the detection of theophylline (Table 1). A lower

Table 1 Summary of different immobilisation methods for unmodified MIP particles onto conductive electrodes devices/biosensors with MIP materials for theophylline and related compounds

Template	Monomer composition	Polymer type	Immobilisation method	Sensing principle	LOD	Operational lifetime	Reference
Hydroquinone	MAA/TRIM	Macroporous microsphere	Agarose gel on glassy carbon electrode	Voltammetry	1 μM	N/A	[20]
1-hydroxypyrene	Styrene/DVB	Macroporous microsphere	Carbon ink on screen printed electrode	Voltammetry	0.1 mM	N/A	[39]
Caffeine	MAA/EGDMA	Monolith	Integrated in carbon paste electrode	Voltammetry	0.6 nM	N/A	[13]
Theophylline	MAA/EGDMA	Film	Adhered layer	Surface Plasmon resonance	0.2 mM	N/A	[40]
Theophylline	Electropolymerized phenol	Conducting polymer	Electropolymerization	Capacitance	1 μM	N/A	[41]
Theophylline	Poly (acrylic acid)	Layer by layer	Langmuir-Blodgett film	Gravimetric	N/A	N/A	[42]
Theophylline	Electropolymerized phenylenediamine+ gold nanoparticles	Conducting polymer	Electropolymerization	Voltammetry	3 μM	N/A	[43]
Theophylline	Electropolymerized polypyrrole	Conducting polymer	Electropolymerization	Gravimetric	1 μM	N/A	[44]
Theophylline	MAA/ ethylene glycol maleic rosinate acrylate	Film	Direct polymerization	Voltammetry	0.1 μM	N/A	[45]
Theophylline	MAA/EGDMA	Macroporous microsphere	Sol–gel on carbon paste electrode	Voltammetry	1 μM	40 cycles	this work

LOD was not possible to confirm due to the increasingly poor signal-to-noise ratio thought to be caused by interference originating from the aforementioned background currents created by the graphite electrode, inherent to the detection of methylxanthines. The authors believe that lower LOD would be possible with the incorporation of a conducting core into the MIP particles during their synthesis so as to augment the signal within the sensor rather than in the solution.

Conclusions

A MIP-incorporating voltammetric sensor, responsive to the alkaloid theophylline has been presented. A modified sol–gel protocol was exploited to immobilize MIP microspherical particles onto epoxy-graphite electrodes which were synthesised in-house. Primary response, cross response to other alkaloids, 1,7-dimethylxanthine, caffeine and theobromine, and electrode regeneration was investigated using DPV. The preferential occupation of the surface of the sol–gel membrane by the MIP particles allowed both a quick measurement time and regeneration of the electrode. It was found a limit of detection consistent with sensors incorporating similarly synthesised MIP particles using chronoamperometry. To the authors' knowledge, this is the first report of a standard methacrylate-based MIP being used for quantitative electrochemical measurements using sol–gel immobilization methods.

Acknowledgments This research was supported by the Research Executive Agency (REA) of the European Union under Grant Agreement number PITN-GA-2010-264772 (ITN CHEBANA), by the Ministry of Science and Innovation (MCINN, Madrid, Spain) through the project CTQ2010-17099 and by the Catalonia program ICREA Academia.

References

1. Mello LD, Kubota LT (2002) Review of the use of biosensors as analytical tools in the food and drink industries. Food Chem 77(2): 237–256
2. Kroger S, Turner APF, Mosbach K, Haupt K (1999) Imprinted polymer based sensor system for herbicides using differential-pulse voltammetry on screen printed electrodes. Anal Chem 71(17):3698–3702
3. Wulff G (2013) Fourty years of molecular imprinting in synthetic polymers: origin, features and perspectives. Microchim Acta 180(15–16):1359–1370
4. Whitcombe MJ, Kirsch N, Nicholls IA (2014) Molecular imprinting science and technology: a survey of the literature for the years 2004–2011. J Mol Recog 27(6):297–401
5. Yan HY, Row KH (2006) Characteristic and synthetic approach of molecularly imprinted polymer. Int J Mol Sci 7(5–6):155–178
6. Wulff G, Knorr K (2001) Stoichiometric noncovalent interaction in molecular imprinting. Bioseparation 10(6):257–276
7. Yoshimi Y, Ohdaira R, Iiyama C, Sakai K (2001) "Gate effect" of thin layer of molecularly-imprinted poly (methacrylic acid-co-ethyleneglycol dimethacrylate). Sensors Actuators B Chem 73(1): 49–53
8. Sellergren B (1997) Noncovalent molecular imprinting: antibody-like molecular recognition in polymeric network materials. Trac-Trend Anal Chem 16(6):310–320
9. Cormack PAG, Elorza AZ (2004) Molecularly imprinted polymers: synthesis and characterisation. J Chromatogr B 804(1): 173–182
10. Suryanarayanan V, Wu CT, Ho KC (2010) Molecularly imprinted electrochemical sensors. Electroanalysis 22(16):1795–1811
11. Sellergren B, Shea KJ (1995) Origin of peak asymmetry and the effect of temperature on solute retention in enantiomer separations on imprinted chiral stationary phases. J Chromatogr A 690(1):29–39
12. Barnes PJ (2010) Theophylline. Pharma 3(3):725–747
13. Alizadeh T, Ganjali MR, Zare M, Norouzi P (2010) Development of a voltammetric sensor based on a molecularly imprinted polymer (MIP) for caffeine measurement. Electrochim Acta 55(5):1568–1574
14. Ebarvia BS, Binag CA, Sevilla F 3rd (2004) Biomimetic piezoelectric quartz sensor for caffeine based on a molecularly imprinted polymer. Anal Bioanal Chem 378(5):1331–1337
15. Aranda M, Morlock G (2007) Simultaneous determination of caffeine, ergotamine, and metamizol in solid pharmaceutical formulation by HPTLC-UV-FLD with mass confirmation by online HPTLC-ESI-MS. J Chromatogr Sci 45(5):251–255
16. Tzanavaras PD, Themelis DG (2007) Development and validation of a high-throughput high-performance liquid chromatographic assay for the determination of caffeine in food samples using a monolithic column. Anal Chim Acta 581(1):89–94
17. Svorc L (2013) Determination of caffeine: a comprehensive review on electrochemical methods. Int J Electrochem Sci 8(4):5755–5773
18. Spataru N, Sarada BV, Tryk DA, Fujishima A (2002) Anodic voltammetry of xanthine, theophylline, theobromine and caffeine at conductive diamond electrodes and its analytical application. Electroanalysis 14(11):721–728
19. Perez-Moral N, Mayes AG (2004) Comparative study of imprinted polymer particles prepared by different polymerisation methods. Anal Chim Acta 504(1):15–21
20. Kan X, Zhao Q, Zhang Z, Wang Z, Zhu JJ (2008) Molecularly imprinted polymers microsphere prepared by precipitation polymerization for hydroquinone recognition. Talanta 75(1):22–26
21. Adhikari B, Majumdar S (2004) Polymers in sensor applications. Prog Polym Sci 29(7):699–766
22. Kriz D, Mosbach K (1995) Competitive amperometric morphine sensor-based on an agarose immobilized molecularly imprinted polymer. Anal Chim Acta 300(1–3):71–75
23. Patel AK, Sharma PS, Prasad BB (2009) Electrochemical sensor for uric acid based on a molecularly imprinted polymer brush grafted to tetraethoxysilane derived sol–gel thin film graphite electrode. Mater Sci Eng C 29(5):1545–1553
24. Prasad BB, Madhuri R, Tiwari MP, Sharma PS (2010) Electrochemical sensor for folic acid based on a hyperbranched molecularly imprinted polymer-immobilized sol–gel-modified pencil graphite electrode. Sensors Actuators B Chem 146(1):321–330
25. Takagishi T, Klotz IM (1972) Macromolecule-small molecule interactions - introduction of additional binding-sites in polyethyleneimine by disulfide crosslinkages. Biopolymers 11 (2): 483-&
26. Mujahid A, Lieberzeit PA, Dickert FL (2010) Chemical sensors based on molecularly imprinted sol–gel materials. Mater 3(4): 2196–2217
27. Ye L, Weiss R, Mosbach K (2000) Synthesis and characterization of molecularly imprinted microspheres. Macromolecules 33(22):8239–8245

28. Ocaña C, Arcay E, del Valle M (2014) Label-free impedimetric aptasensor based on epoxy-graphite electrode for the recognition of cytochrome c. Sensors Actuators B Chem 191:860–865
29. Patel AK, Sharma PS, Prasad BB (2008) Development of a creatinine sensor based on a molecularly imprinted polymer-modified sol–gel film on graphite electrode. Electroanalysis 20(19):2102–2112
30. Sherrington DC (1998) Preparation, structure and morphology of polymer supports. Chem Commun 21:2275–2286
31. Castell OK, Allender CJ, Barrow DA (2006) Novel biphasic separations utilising highly selective molecularly imprinted polymers as biorecognition solvent extraction agents. Biosens Bioelectron 22(4): 526–533
32. Mohamed MH, Wilson LD (2012) Porous copolymer resins: tuning pore structure and surface area with non reactive porogens. Nanomater 2(2):163–186
33. Patel AK, Sharma PS, Prasad BB (2009) Electrochemical sensor for uric acid based on a molecularly imprinted polymer brush grafted to tetraethoxysilane derived sol–gel thin film graphite electrode. Mat Sci Eng C-Bio S 29(5):1545–1553
34. Patel AK, Sharma PS, Prasad BB (2009) Voltammetric sensor for barbituric acid based on a sol-gel derivated molecularly imprinted polymer brush grafted to graphite electrode Int J Pharm 371(1–2): 47–55
35. Liu J, Chaudhury MK, Berry DH, Seebergh JE, Osborne JH, Blohowiak KY (2006) Effect of surface morphology on crack growth at a sol–gel reinforced epoxy/aluminum interface. J Adhes 82(5): 487–516
36. Viana MM, Mohallem TDS, Nascimento GLT, Mohallem NDS (2006) Nanocrystalline titanium oxide thin films prepared by sol–gel process. Braz J Phys 36(3B):1081–1083
37. Brittain HG (2007) Profiles of drug substances, excipients and related methodology: critical compilation of pKa values for pharmaceutical substances, vol 33. Academic, San Diego CA
38. Castell OK, Barrow DA, Kamarudin AR, Allender CJ (2011) Current practices for describing the performance of molecularly imprinted polymers can be misleading and may be hampering the development of the field. J Mol Recog 24(6):1115–1122
39. Kirsch N, Hart JP, Bird DJ, Luxton RW, McCalley DV (2001) Towards the development of molecularly imprinted polymer based screen-printed sensors for metabolites of PAHs. Analyst 126(11): 1936–1941
40. Lai EPC, Fafara A, VanderNoot VA, Kono M, Polsky B (1998) Surface plasmon resonance sensors using molecularly imprinted polymers for sorbent assay of theophylline, caffeine, and xanthine. Can J Chem 76(3):265–273
41. Wang Z, Kang J, Liu X, Ma Y (2007) Capacitive detection of theophylline based on electropolymerized molecularly imprinted polymer. Int J Polym Anal Charact 12(2):131–142
42. Niu J, Liu Z, Fu L, Shi F, Ma H, Ozaki Y, Zhang X (2008) Surface-imprinted nanostructured layer-by-layer film for molecular recognition of theophylline derivatives. Langmuir 24(20):11988–11994
43. Kan X, Liu T, Zhou H, Li C, Fang B (2010) Molecular imprinting polymer electrosensor based on gold nanoparticles for theophylline recognition and determination. Microchim Acta 171(3–4):423–429
44. Kim J-M, Lee U-H, Chang S-M, Park JY (2014) Gravimetric detection of theophylline on pore-structured molecularly imprinted conducting polymer. Sensors Actuators B Chem 200:25–30
45. Tan X, Wang L, Li P, Gong Q, Liu L, Zhao D, Lei F, Huang Z (2012) Electrochemical sensor for the determination of theophylline based on molecularly imprinted polymer with ethylene glycol maleic rosinate acrylate as cross-linker. Acta Chim Sin 70(9):1088–1094